

1 **Title: Neutrophils prime unique transcriptional responses in intestinal organoids**  
2 **during infection with nontyphoidal *Salmonella enterica* serovars**

3

4 **Authors/Affiliations**

5 Anna-Lisa E. Lawrence<sup>1</sup>, Ryan P. Berger<sup>1</sup>, David R. Hill<sup>2</sup>, Sha Huang<sup>3</sup>, Veda K. Yadagiri<sup>2</sup>,  
6 Brooke Bons<sup>2</sup>, Courtney Fields<sup>2</sup>, Jason S. Knight<sup>2</sup>, Christiane E. Wobus<sup>1</sup>, Jason R.  
7 Spence<sup>3</sup>, Vincent B. Young<sup>1,2</sup>, Basel H. Abuaita<sup>1,a,b</sup>, and Mary X. O'Riordan<sup>1a</sup>

8

9 <sup>1</sup> Department of Microbiology and Immunology, University of Michigan Medical School,  
10 Ann Arbor, MI, USA

11 <sup>2</sup> Department of Internal Medicine/Infectious Diseases Division, University of Michigan  
12 Medical School, Ann Arbor, MI, USA

13 <sup>3</sup> Department of Cell and Developmental Biology, University of Michigan Medical School,  
14 Ann Arbor, MI, USA

15

16 **Author list footnotes**

17 <sup>a</sup> M.X.O and B.H.A contributed equally to the work

18 <sup>b</sup> B.H.A Present address: Department of Pathobiological Sciences, Louisiana State  
19 University School of Veterinary Medicine, Baton Rouge, LA, USA

20

21 **Contact Info**

22 **\*Correspondence:** [babuaita@lsu.edu](mailto:babuaita@lsu.edu), [oriordan@umich.edu](mailto:oriordan@umich.edu)

23

24 **Abstract:**

25 Nontyphoidal strains of *Salmonella enterica* are a major cause of foodborne illnesses and  
26 infection with these bacteria result in inflammatory gastroenteritis. Neutrophils are a  
27 dominant immune cell type found at the site of infection in *Salmonella*-infected individuals,  
28 but how they regulate infection outcome is not well understood. Here we used a co-culture  
29 model of primary human neutrophils and human intestinal organoids to probe the role of  
30 neutrophils during infection with two of the most prevalent *Salmonella* serovars:  
31 *Salmonella enterica* serovar Enteritidis and Typhimurium. Using a transcriptomics  
32 approach, we identified a dominant role for neutrophils in mounting differential immune  
33 responses including production of pro-inflammatory cytokines, chemokines, and  
34 antimicrobial peptides. We also identified specific gene sets that are induced by  
35 neutrophils in response to Enteritidis or Typhimurium infection. By comparing host  
36 responses to these serovars, we uncovered differential regulation of host metabolic  
37 pathways particularly induction of cholesterol biosynthetic pathways during Typhimurium  
38 infection and suppression of RNA metabolism during Enteritidis infection. Together these  
39 findings provide insight into the role of human neutrophils in modulating different host  
40 responses to pathogens that cause similar disease in humans.

41

42 **Importance:**

43 Nontyphoidal serovars of *Salmonella enterica* are known to induce robust neutrophil  
44 recruitment in the gut during early stages of infection, but the specific role of neutrophils  
45 in regulating infection outcome of different serovars is poorly understood. Due to  
46 differences in human infection progression compared to small animal models,

47 characterizing the role of neutrophils during infection has been challenging. Here we used  
48 a co-culture model of human intestinal organoids with human primary neutrophils to study  
49 the role of neutrophils during infection of human intestinal epithelium. Using a  
50 transcriptomics approach, we define neutrophil-dependent reprogramming of the host  
51 response to *Salmonella*, establishing a clear role in amplifying pro-inflammatory gene  
52 expression. Additionally, the host response driven by neutrophils differed between two  
53 similar nontyphoidal *Salmonella* serovars. These findings highlight the importance of  
54 building more physiological infection models to replicate human infection conditions to  
55 study host responses specific to individual pathogens.

56

57 **Introduction:**

58 Foodborne illnesses account for an estimated 48 million infections in the United States  
59 every year with 128,000 individuals needing to be hospitalized (1). One of the most  
60 common causes of foodborne disease is *Salmonella enterica*, which is responsible for an  
61 estimated 1.35 million infections in the United States each year (2). *Salmonella enterica*  
62 is comprised of over 2500 different serovars with *Salmonella enterica* serovar  
63 Typhimurium (STM) and Enteritidis (SE) among the most prevalent serovars globally.  
64 *Salmonella enterica* infects via the fecal-oral route and once it reaches the intestinal tract  
65 it stimulates a strong inflammatory response from the host leading to gastroenteritis and  
66 diarrheal disease (3). Although these symptoms are usually self-resolving, individuals  
67 with compromised immune systems or malnutrition can experience severe systemic,  
68 sometimes fatal, illness (4).

69

70 *Salmonella* pathogenesis is commonly studied *in vivo* using inbred mouse models.  
71 Notably, disease progression caused by *Salmonella* is often different in mice compared  
72 to humans, including the fact that mice rarely develop diarrhea during these infections  
73 (5). To better understand human infection, human-derived cells including human intestinal  
74 organoids (HIOs) have been used to define human-specific host responses to *Salmonella*  
75 (6–8). HIOs are derived from human pluripotent stem cells and self-organize to form a 3-  
76 dimensional polarized epithelium with differentiated epithelial cells and an underlying  
77 mesenchyme (9). Bacteria, including *Salmonella*, are able to replicate and stimulate  
78 robust inflammatory responses in HIOs (6–8, 10–12). Although the HIO model and other  
79 tissue culture models have been invaluable in revealing human-specific responses to  
80 *Salmonella* infection (6–8, 13–15), key features missing from these models are known to  
81 shape the outcome of infection, including immune cells.

82  
83 Several immune cell types contribute to the control and resolution of *Salmonella*  
84 infections, however one of the earliest responders and the most abundant cell type found  
85 in *Salmonella*-infected individuals are polymorphonuclear leukocytes (PMNs), specifically  
86 neutrophils (16, 17). PMNs defend against bacterial infections through both cell-intrinsic  
87 and -extrinsic mechanisms - antimicrobial effectors like degradative proteases and ion  
88 chelators, production of reactive oxygen species and formation of sticky antimicrobial  
89 neutrophil extracellular traps (NETs) can directly kill bacteria (18,19)). PMNs also can  
90 influence surrounding cells and tissues, including the intestinal epithelium, changing the  
91 microenvironment via molecular oxygen depletion, regulating nutrient availability, and  
92 through production of inflammatory mediators (20, 21). How the interaction between

93 intestinal epithelial cells and PMNs affect the outcome of bacterial infections is still poorly  
94 understood. To address this gap in knowledge, we generated a PMN-HIO model by co-  
95 culturing primary human PMNs with HIOs that were infected with *Salmonella enterica*  
96 serovar Enteritidis (SE) or Typhimurium (STM) by microinjection of bacteria into the  
97 lumen. Using this PMN-HIO model, we characterized how PMNs modulate intestinal  
98 epithelial host defenses during infection, compared to HIOs alone. We show here that the  
99 presence of PMNs elevates intestinal epithelial proinflammatory signaling, including  
100 production of cytokines, chemokines, and antimicrobial effectors. PMN-HIOs also  
101 distinguished between the two serovars through differential upregulation of metabolic  
102 pathways indicating that there are additional nuances in how PMN-HIOs respond to  
103 different pathogens.

104

105 **Results:**

106 **PMNs enhance HIO immune activation and other transcriptional responses during**  
107 ***Salmonella* infection**

108 PMNs are potent drivers of inflammation, so we reasoned that PMNs would likely  
109 modulate the intestinal host response to *Salmonella* infection. Using the PMN-HIO model,  
110 we previously characterized the degree of PMN recruitment and effect on bacterial  
111 colonization during *Salmonella* infection (22). Here, to probe the contribution of PMNs to  
112 the global intestinal transcriptional responses during infection, HIOs and PMN-HIOs were  
113 microinjected with SE, STM or PBS and harvested at 8h post-infection (8hpi) for bulk  
114 RNA-sequencing (RNA-seq). Principal component analysis (PCA) was performed on  
115 normalized gene counts to determine whether PMNs drove separation between HIOs and

116 PMN-HIOs and therefore changed the transcriptional profile during infection (Fig. 1A).  
117 While there was definitive segregation between infected HIOs in the presence and  
118 absence of PMNs, there was no clear separation between PBS control HIOs and PMN-  
119 HIOs, suggesting that PMNs change the transcriptional profile of the HIOs only during  
120 infection. To determine which biological pathways contributed most to the segregation  
121 between HIOs and PMN-HIOs, we extracted the loadings data from principal component  
122 1 and subjected the top 50 genes to pathway enrichment analysis in Reactome to identify  
123 biological processes that these genes participate in (Fig. 1B). Approximately 75% of these  
124 genes belonged to the immune system, disease processes, and signal transduction  
125 suggesting a dominant role of immune activation for PMNs in the PMN-HIO model.  
126 Collectively, these data support that PMNs induce changes in HIO responses only during  
127 infection and that PMNs primarily induce enrichment of immune-related pathways.

128  
129 To further analyze which specific processes were induced by PMNs and how these  
130 pathways were enriched under various culture conditions, we performed pathway  
131 enrichment analysis of these top pathways with all genes that had a p-adjusted value  
132 <0.05 relative to control PBS-injected HIOs (Fig. 1C, and Table S1). Each pathway was  
133 analyzed for gene ratio (fraction of genes in a pathway that were significantly changed  
134 relative to total genes in that pathway) plotted on the x-axis, and the statistical  
135 significance, depicted as dot size, based on  $-\log_{10}(p\text{-adjusted})$ . As anticipated, immune  
136 system-related pathways were among the most significantly enriched pathways in  
137 response to infection (Fig. 1C). These included pathways belonging to processes  
138 involving signaling by interleukins, Toll-like receptor signaling, as well as PMN-specific

139 pathways like neutrophil degranulation. We also detected enrichment of signal  
140 transduction pathways that also relate to PMN function. These pathways were related to  
141 Rho GTPase signaling. Activation of Rho GTPases has been shown in numerous studies  
142 to be critical in membrane remodeling during *Salmonella* infection and are targeted by  
143 secreted *Salmonella* effectors (23). Taken together, these results highlight the viability of  
144 the PMN-HIO model, demonstrating that neutrophils enhance the inflammatory tone of  
145 the HIO in an infection-specific manner.

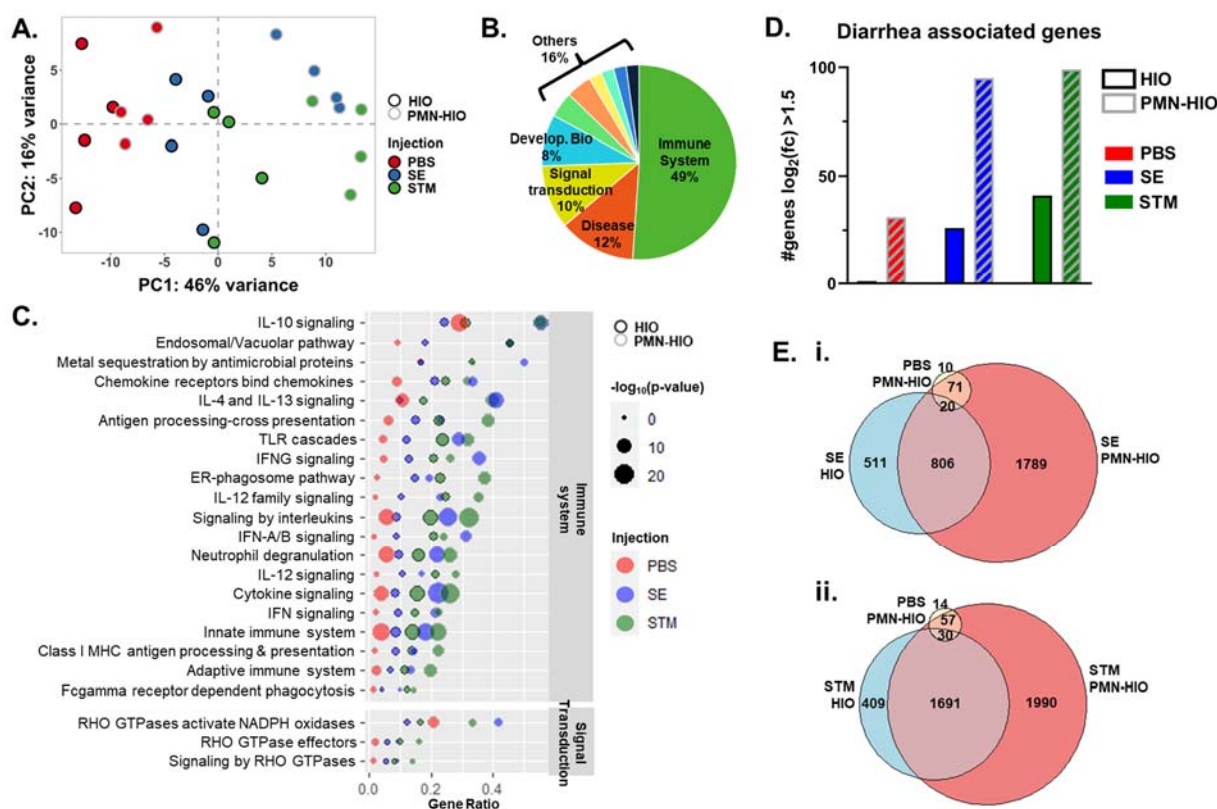
146

147 One hallmark of infection with nontyphoidal *Salmonella* serovars is the development of  
148 inflammatory diarrhea. Since many of the top genes driving segregation between PMN-  
149 HIOs and HIOs were related to immune system processes, we assessed infected HIOs  
150 and PMN-HIOs for enrichment of genes associated with diarrhea (24). As predicted, the  
151 number of diarrhea-associated genes that were significantly changed increased with  
152 infection (Fig 1D). Consistent with our findings that PMNs upregulate immune pathways,  
153 the number of diarrhea-associated genes further increased in infected PMN-HIOs  
154 compared to infected HIOs. PMNs also appeared to increase the fold change of many  
155 genes that were changed in infected HIOs. These results suggest that PMNs not only  
156 amplify inflammatory processes during intestinal infection but may also promote induction  
157 of diarrhea.

158

159 To investigate how PMNs changed the HIO response during infection at the gene level,  
160 significant gene changes were calculated relative to PBS control HIOs and filtered for  
161 adjusted p-value <0.05 (Table S2). Venn diagrams were generated to compare gene

162 changes during SE infection +/- PMNs or STM infection +/-PMNs (Fig. 1E). Although a  
 163 substantial number of genes were changed during infection in both HIOs and PMN-HIOs,  
 164 over 1700 additional genes were induced in SE-infected PMN-HIOs and over 1900 in  
 165 STM-infected PMN-HIOs relative to HIOs alone. Importantly, there were very few genes  
 166 induced in PBS control PMN-HIOs, confirming that adding PMNs to the HIOs alone does  
 167 not trigger major changes in transcriptional programming, but the complex interaction  
 168 between PMNs, HIOs and *Salmonella* drove a robust transcriptional response. Together  
 169 these results demonstrate that co-culture with PMNs amplifies the HIO response to  
 170 *Salmonella* infection including expression of genes that were not induced in infected HIOs  
 171 alone, as well as enhanced enrichment of immune-related processes.



172

173 **Fig 1. PMNs enhance HIO immune activation and other transcriptional responses during**  
 174 ***Salmonella* infection**

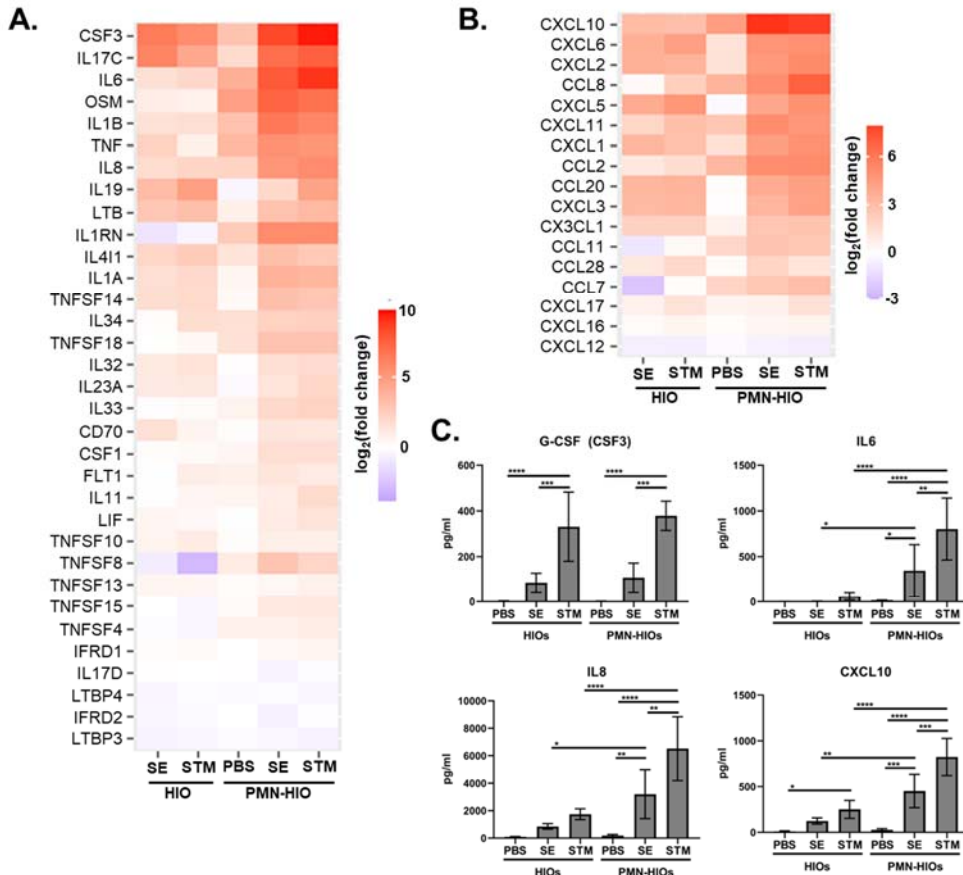
175 A. PCA plot of HIOs and PMN-HIOs infected with STM or SE with PBS as the mock control for 8h.  
 176 B. Loadings data from PC1 was extracted from A to identify the top 50 genes driving separation

177 of samples via PC1. Genes were then assessed for pathway enrichment using the Reactome  
178 database. Pie chart shows the percent of the top 50 pathways belonging to each of the Major  
179 Reactome pathway categories C. Dot plot assessing pathway enrichment of the top 50 identified  
180 pathways in (B) using all differentially expressed genes (p-adjusted value<0.05 compared to PBS-  
181 injected HIOs). Gene ratio is shown on the x-axis and the dot size corresponds to the -log10(p-  
182 value). HIO samples are outlined in black while PMN-HIOs are outlined in gray. PBS-injection  
183 (red), SE-injection (blue), STM-injection (green). D. Number of diarrhea associated genes with p-  
184 adjusted <0.05 and log<sub>2</sub>(fold change)>1.5 in each condition. Gene list for this analysis was used  
185 from (23). E. Venn diagram comparing differentially regulated genes with p-adjusted value <0.05  
186 relative to PBS-injected HIOs for SE-injected HIOs, PBS-injected PMN-HIOs, and SE-injected  
187 PMN-HIOs (i.) and STM-injected HIOs, PBS-injected PMN-HIOs and STM-injected PMN-HIOs  
188 (ii.).

189 **PMNs elevate production of cytokines and chemokines in the PMN-HIOs**

190 We recently reported that both SE and STM induce robust pro-inflammatory signaling in  
191 the HIO through transcriptional upregulation of cytokine and chemokine genes and  
192 downstream secretion of these effectors (6, 8). Because we observed a further increase  
193 in pathway enrichment of several pro-inflammatory pathways in the infected PMN-HIOs  
194 compared to infected HIOs, we examined the contribution of PMNs in changing  
195 expression and production of some of these pro-inflammatory mediators including  
196 cytokines and chemokines. Consistent with pathway enrichment results, PMN-HIOs  
197 increased expression of almost every cytokine and chemokine that was significantly  
198 changed during either SE or STM infection in the HIOs alone (Fig. 2A-2B). This elevated  
199 PMN-dependent response was primarily driven by infection, as there was little  
200 upregulation of these genes in PBS control PMN-HIOs. Of interest, in infected PMN-HIOs,  
201 we observed increased transcript levels of cytokines CSF-3, IL-6, IL-8 (Fig. 2A) and  
202 chemokines CXCL-10 and CCL-2 (Fig. 2B), all of which are essential for progression and  
203 resolution of intestinal inflammation (25–27). To assess whether these transcriptional  
204 changes were reflected at the protein level, supernatants from HIOs and PMN-HIOs were  
205 collected for ELISA to measure cytokine and chemokine output (Fig. 2C). Protein level  
206 analyses revealed similar patterns to the transcriptional results. Overall, the production of

207 most cytokines and chemokines in infected PMN-HIOs was increased compared to  
208 infected HIOs or uninfected PMN-HIO controls. This included significant increases in IL-  
209 6, IL-8, CXCL-10, and CCL-2 production in infected PMN-HIOs compared to infected  
210 HIOs. However, some cytokines such as G-CSF (encoded by *CSF3*) or CXCL-2 did not  
211 significantly change with the addition of PMNs. While most other pro-inflammatory  
212 proteins correlated well with the transcript data, *CSF3* transcript was dramatically  
213 upregulated in infected PMN-HIOs, compared to infected HIOs, even though there was  
214 no difference in secreted protein levels. It is notable that although SE and STM induce  
215 similar degrees of *CSF3* transcript upregulation, protein levels of G-CSF in the  
216 supernatant are significantly lower in SE-infected PMN-HIOs compared to STM,  
217 suggesting that SE may regulate G-CSF post-transcriptionally. All together, we found that  
218 inflammatory signaling was elevated when PMNs are present in infected HIOs.



219

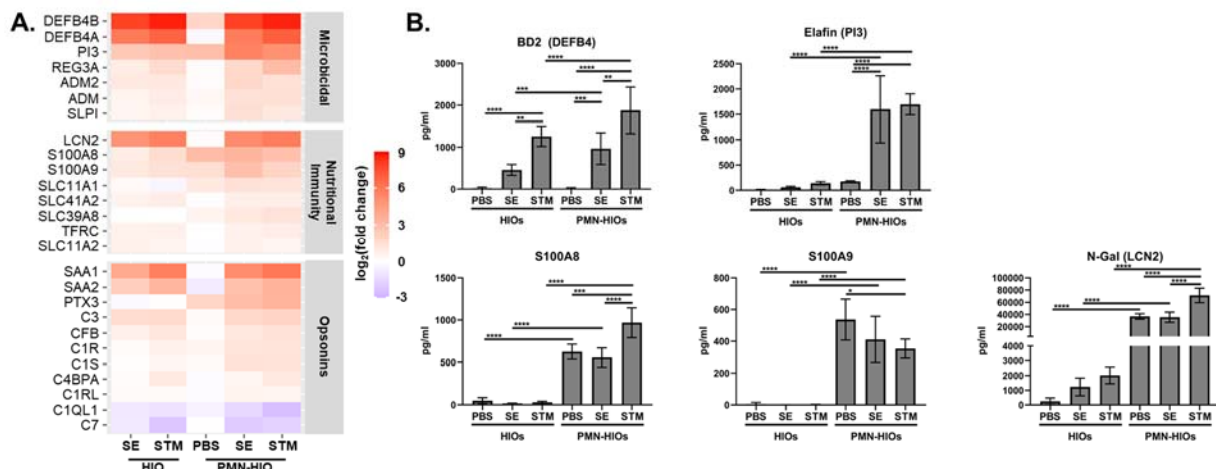
220 **Fig 2. PMN-HIO co-culture amplifies production of cytokines and chemokines in infected**  
221 **HIOs**

222 A-B. Gene expression data presented as  $\log_2(\text{fold change})$  relative to PBS-injected HIOs for (A)  
223 cytokines and (B) chemokines. Genes that were significantly changed from PBS-injected HIOs in  
224 at least one condition with  $p$ -adjusted  $<0.05$  are included. C. ELISA data from culture media  
225 sampled at 8hpi with 5 HIOs per well with  $n=4$  replicates. Significance was determined by 2-way  
226 ANOVA where \* $p<0.05$ , \*\* $p<0.01$ , \*\*\* $p<0.001$ , \*\*\*\* $p<0.0001$ .

227 **HIO co-culture with PMNs strengthens the antimicrobial environment**

228 Antimicrobial effectors such as defensins are a key component of the host defense in the  
229 intestine and our previous work demonstrated that antimicrobial peptides (AMPs) are  
230 strongly upregulated during infection in the HIO model (6, 8). Among the pathways  
231 enriched (Fig. 1C), was 'metal sequestration by antimicrobial proteins' suggesting that  
232 PMNs strongly affect the antimicrobial milieu in the HIOs. PMNs are known to have a  
233 wide arsenal of antimicrobial effectors, but specifically how PMNs affect the antimicrobial

234 response during infection in complex environments such as in the PMN-HIO model has  
235 not been fully defined. In contrast to what we had predicted, PMNs did not dramatically  
236 enhance transcriptional upregulation of antimicrobial effectors above what was observed  
237 in infected HIOs. This included beta-defensins (DEFB4A/B), nutritional immunity effectors  
238 such as lipocalin (LCN2) or calprotectin (S100A8/9), and opsonins like SAA1/2 (Fig. 3A),  
239 which were all highly upregulated during infection in both HIOs and PMN-HIOs. Since  
240 PMNs represent approximately less than 5% of the cells in the PMN-HIO model (22), the  
241 contribution of PMN transcripts in the overall bulk-RNA-seq is likely minimal. However,  
242 analysis of culture supernatants via ELISA revealed that all these mediators were present  
243 at significantly higher levels in infected PMN-HIOs compared to HIOs (Fig. 3B). Some of  
244 these effectors were responsive to infection stimuli including beta-defensin (BD2,  
245 encoded by DEFB4A and DEFB4B) and elafin (encoded by PI3) as they were not present  
246 at high concentrations in the uninfected controls. In contrast, the nutritional immunity  
247 effectors calprotectin and lipocalin were constitutively produced by PMNs, whether HIOs  
248 were injected with PBS or *Salmonella*. Collectively, transcript and protein analyses of  
249 infected PMN-HIOs reveal that a small population of neutrophils can substantially  
250 enhance the antimicrobial environment.



251

### 252 **Fig 3. Presence of PMNs strengthens the antimicrobial environment**

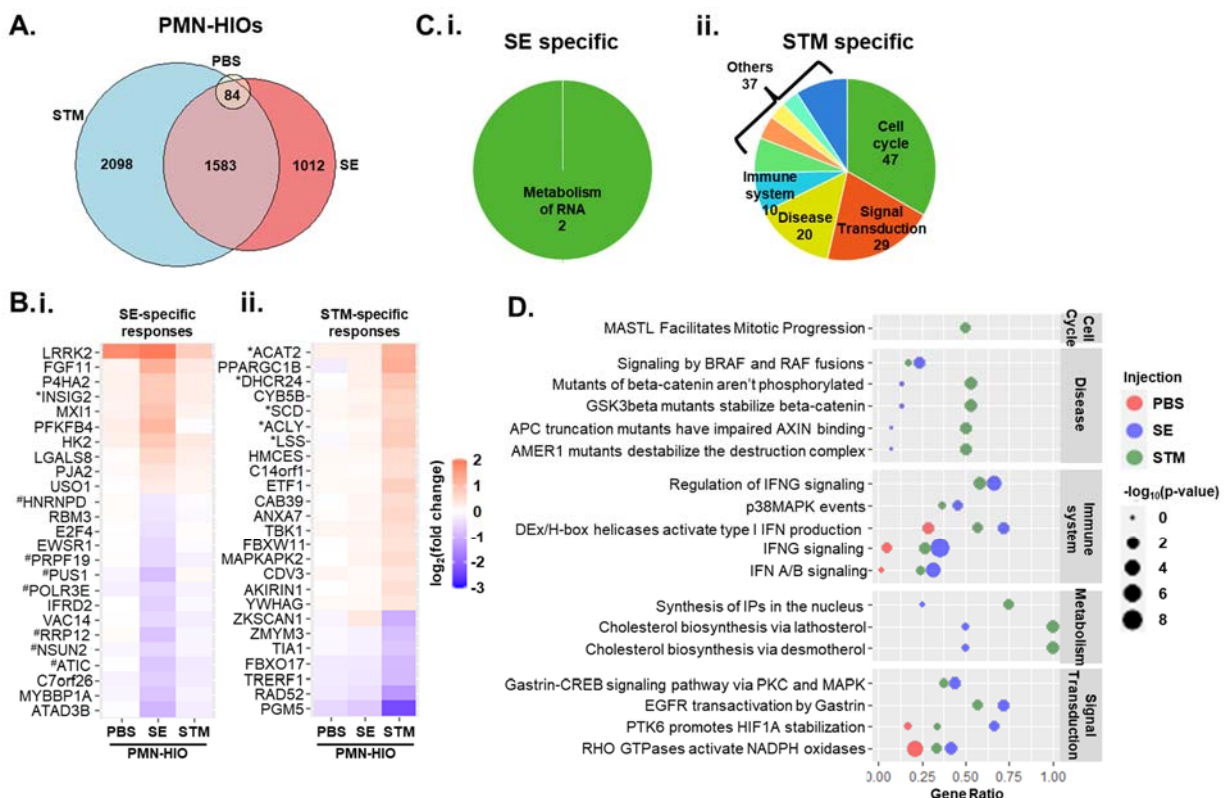
253 A. Gene expression data presented as log2(fold change) relative to PBS-injected HIOs for  
254 antimicrobial genes. Heatmap is divided into functional categories: Microbicidal, Nutritional  
255 Immunity, and Opsonins. Genes that were significantly changed from PBS-injected HIOs in at  
256 least one condition with p-adjusted <0.05 are included. B. ELISA data from culture media sampled  
257 at 8hpi with 5 HIOs per well with n=4 replicates. Significance was determined by 2-way ANOVA  
258 where \*p<0.05, \*\*p<0.01, \*\*\*p<0.001, \*\*\*\*p<0.0001.

### 259 **PMN-HIOs induce unique responses to two nontyphoidal *Salmonella* serovars**

260 SE and STM share high levels of gene homology but accessory genes unique to SE  
261 contribute to its pathogenesis in a mouse model of infection (28–30). We also found that  
262 these serovars elicit unique responses by human intestinal epithelium (8). Consistent with  
263 this earlier finding, we observed clustering of SE-infected PMN-HIOs away from STM-  
264 infected PMN-HIOs via principal component analysis (PC2) (Fig. 1A). These data suggest  
265 that PMN-HIOs also mount distinct responses to these two serovars. To characterize  
266 these responses, significant genes from SE, STM, and PBS-injected PMN-HIOs were  
267 compared to determine the overlap in transcriptional responses to infection (Fig. 4A).  
268 Surprisingly, while there was a core set of host genes that were changed in response to  
269 both SE and STM, the majority of genes were uniquely induced by only one serovar with  
270 over 1000 genes uniquely changed during SE-infection of the PMN-HIOs and over 2000  
271 genes uniquely changed during STM-infection. To better characterize the functional

272 differences in these responses, the top 25 significant genes that were changed in either  
273 SE-infected or STM-infected PMN-HIOs were plotted and assessed for fold change  
274 relative to PBS-injected HIOs (Fig. 4B). The genes that were uniquely changed during  
275 SE-infection belonged to multiple biological processes including metabolism (PFKFB4  
276 and HK2) although RNA modification-related genes were highly represented among the  
277 downregulated genes (ATIC, RRP12, NSUN2, and PUS1). More genes were  
278 downregulated in SE-infected PMN-HIOs compared to STM-infected PMN-HIOs where  
279 most genes that were uniquely responding to STM were upregulated. While these genes  
280 also fell into multiple categories, upregulation of cholesterol biosynthetic genes in STM-  
281 infected PMN-HIOs were highly prevalent in this heatmap (ACAT2, DHCR24, SCD,  
282 ACLY, and LSS). To further characterize which pathways were differentially induced  
283 during infection with the two serovars, pathway enrichment analysis on uniquely regulated  
284 genes identified in Fig. 4A was performed. To classify these pathways into different  
285 biological processes, each significantly enriched pathway was mapped back to the parent  
286 pathway in the Reactome database (Fig. 4C, Tables S3 and S4). Out of the 1012 genes  
287 that were uniquely induced in SE-infected PMN-HIOs, only 2 pathways were significantly  
288 enriched: 'metabolism of RNA' and 'rRNA modification'. Most of the genes differentially  
289 expressed only during SE infected were downregulated (Fig. 4B). In contrast, 143  
290 Reactome pathways were enriched in STM-infected PMN-HIOs representing a much  
291 more diverse set of biological processes. Cell cycle-related and signal transduction  
292 pathways were all highly represented among genes that were only induced in STM-  
293 infected PMN-HIOs, but we also noted that additional genes belonging to immune system  
294 pathways were uniquely induced in STM-infected PMN-HIOs leading to higher

295 enrichment of these pathways. These findings suggest that while both serovars trigger  
296 different responses by PMN-HIOs, responses unique to SE infection largely relate to RNA  
297 metabolism while STM induces a broad range of host cell responses. Lastly, to compare  
298 pathway enrichment across all differentially expressed genes, pathways that were  
299 significant in either SE or STM infected PMN-HIOs were selected and sorted based on  
300 biggest difference in gene ratio between the two serovars (Fig. 4D). Multiple biological  
301 processes were differentially enriched when assessing the entire set of significant genes,  
302 including cell cycle, disease-related processes specifically relating to beta-catenin  
303 stability, immune system and metabolism related pathways. Pathways where SE  
304 exhibited greater gene ratios compared to STM-infected samples were mostly related to  
305 interferon signaling, although the 'HIF1A stabilization' pathway was also more enriched  
306 in SE-infected PMN-HIOs. Most of these pathways were also highly enriched during STM-  
307 infection with only a slight increase in gene ratio in the SE samples suggesting that both  
308 serovars trigger these pathways. In contrast, STM infection resulted in much stronger  
309 enrichment of beta-catenin related pathways and cholesterol biosynthesis pathways.  
310 Sub-pathways of cholesterol biosynthesis, namely biosynthesis via lathosterol and  
311 desmosterol had a gene ratio of 1 in STM-infected PMN-HIOs, meaning that all genes in  
312 these pathways were significantly changed during infection. Overall, our findings reveal  
313 differential responses between infection with SE and STM in the PMN-HIOs, including  
314 regulation of genes involved in RNA modification in SE-infected PMN-HIOs. Host  
315 responses to the two serovars were strikingly different in their stimulation of metabolic  
316 pathways, specifically highly enriched cholesterol biosynthetic pathways observed only in  
317 STM-infected PMN-HIOs.



318

319 **Fig 4. PMN-HIOs distinguish between SE and STM infection**

320 A. Venn diagram comparing differentially regulated genes with p-adjusted value <0.05 relative to  
321 PBS-injected HIOs for STM-injected, SE-injected, or PBS-injected PMN-HIOs. B. Heatmap of  
322 unique differentially expressed genes. Top 25 genes based on adjusted p-value that were  
323 significant in only SE-injected PMN-HIOs (i.) or in STM-injected PMN-HIOs (ii.). Data are  
324 presented as log<sub>2</sub>(fold change) relative to PBS-injected HIOs. \*Cholesterol biosynthetic genes,  
325 #RNA modification genes. C. Pathway enrichment analysis of 1012 SE-induced genes (i.) or 2098  
326 STM-induced genes identified in (A) from the Reactome database. Pie chart shows the number  
327 of each major Reactome pathway category represented by the pathway enrichment results out of  
328 2 significant pathways in SE-infected PMN-HIOs or 143 significant pathways in STM-infected  
329 PMN-HIOs. D. Dot plot assessing pathway enrichment in PMN-HIOs of all differentially expressed  
330 genes (p-adjusted value <0.05 compared to PBS-injected HIOs). Top pathways were selected by  
331 the biggest difference in gene ratio between SE and STM-injected PMN-HIOs. Gene ratio is  
332 shown on the x-axis and the dot size corresponds to the -log<sub>10</sub>(p-value). PBS-injection (red), SE-  
333 injection (blue), STM-injection (green).

334 **Discussion:**

335 PMNs, particularly neutrophils, are early responders to inflammation and represent a  
336 dominant immune cell type recruited to the intestine during infection with nontyphoidal  
337 *Salmonella* serovars. Although it is appreciated that neutrophils are present during the  
338 early phases of *Salmonella* infection, how neutrophils contribute to the host response in

339 a complex microenvironment like the intestine remains poorly understood. Here we used  
340 a transcriptomics approach in a PMN-HIO co-culture model to probe the role of PMNs  
341 during infection with two prevalent serovars of *Salmonella*: *Salmonella enterica* serovar  
342 Enteritidis and Typhimurium. We identified a dominant role for PMNs in enhancing  
343 inflammatory responses, including production of pro-inflammatory cytokines and  
344 chemokines as well as antimicrobial proteins during infection with both serovars. More  
345 broadly, PMNs acted on HIO cells to mount a more complex response to *Salmonella* as  
346 there were over 1000 genes in each infection condition that were uniquely and  
347 differentially expressed in the presence of PMNs. Lastly, we observed distinct responses  
348 between serovars; metabolic pathways were differentially regulated in the PMN-HIOs  
349 during SE and STM infection with robust enrichment of cholesterol biosynthesis genes  
350 during infection with STM, and downregulation of RNA modification-related genes during  
351 SE infection suggesting that PMNs can reprogram the environment in the presence of  
352 different pathogens.

353

354 Infection with nontyphoidal strains of *Salmonella enterica* induce robust inflammatory  
355 responses in the gut leading to gastroenteritis, and although neutrophils are known to be  
356 present at the site of infection, the specific contribution in tuning the inflammatory  
357 environment has been difficult to study in more complex animal models. We found via  
358 RNA-seq, as well as assessing secreted effectors, that the presence of PMNs during  
359 infection increased enrichment of cytokine signaling pathways, increased the  
360 upregulation of several cytokines that were already induced in infected HIOs alone, as  
361 well as led to a significant increase in levels of secreted cytokines and chemokines in the

362 culture supernatants. This pattern was also conserved for antimicrobial effectors including  
363 a PMN-dependent upregulation in bactericidal and nutritional immunity related proteins.  
364 While a subset of these effectors are likely produced by PMNs such as calprotectin  
365 (encoded by S100A8/9) which is known to be highly produced in neutrophils, other  
366 effectors such as beta-defensins (encoded by DEFB4A/B) or elafin (encoded by PI3) are  
367 antimicrobial effectors known to be secreted by epithelial cells (31–33). This pattern would  
368 suggest that PMNs program the epithelium to enhance antimicrobial responses during  
369 infection. This pattern is supported by the prior finding that neutrophil elastase can induce  
370 production of elafin by epithelial cells (34). We also note a dramatic increase in the  
371 number of significant gene changes during infection in PMN-HIOs compared to HIOs,  
372 suggesting that PMNs likely stimulate a broad epithelial response to infection given the  
373 relatively low numbers of neutrophils in the PMN-HIOs. Further work may better elucidate  
374 the specific contribution of each cell type in the response to infection by performing single-  
375 cell RNA-seq, or other single cell approaches.

376

377 PMNs did not function to solely reprogram the inflammatory environment in response to  
378 *Salmonella* infection, but also affected other cellular processes that differentiated  
379 between infecting serovars. We found that over 3000 genes were differentially regulated  
380 during infection with SE and STM in the PMN-HIO model. One of the most striking  
381 differences we observed was transcriptional induction of cholesterol biosynthesis genes  
382 in STM infection of the PMN-HIOs, but not SE infection. In contrast, we noted that SE-  
383 infection uniquely induced upregulation of INSIG2, a negative regulator of cholesterol  
384 biosynthesis. There are numerous reports investigating the role of cholesterol during

385 *Salmonella* infection including affecting invasion into epithelial cells, remodeling of the  
386 *Salmonella* containing vacuole (SCV), bacterial replication, and susceptibility to typhoid  
387 fever (35–43). Although there may be some cell type differences, the overarching pattern  
388 from these studies reveal that increased cholesterol generally enhances *Salmonella*  
389 infection. Our findings that SE does not induce upregulation of cholesterol biosynthetic  
390 genes is intriguing. It is possible that the two serovars have evolved to have a different  
391 dependence on cholesterol for productive infection. Alternatively, redistribution of existing  
392 cholesterol in the cells may be sufficient for SE. We previously reported that SE and STM  
393 exhibit different kinetics in their ability to invade and replicate within HIO epithelial cells,  
394 with SE invading at reduced frequency compared to STM (8). Our findings here point to  
395 cholesterol regulation as a potential mechanism that could contribute to differences in  
396 infection kinetics. Differential regulation of cholesterol biosynthesis as well as other  
397 serovar-specific responses warrant future study to better understand how these closely  
398 related serovars may be interacting with the intestinal epithelium in distinct ways.

399  
400 The findings reported herein lay the groundwork for many future directions. In addition to  
401 PMN-dependent regulation of inflammatory responses and serovar-specific regulation of  
402 cholesterol biosynthesis genes, we also measured a shift in gene expression in response  
403 to *Salmonella* infection by using this co-culture model that was not observed in the HIO  
404 model alone. This included an increase in expression of diarrhea-associated genes.  
405 Modeling diarrheal diseases using mouse models has been difficult since mice rarely  
406 develop diarrhea in response to bacterial infections. Thus, our results open up an area  
407 for future study where the PMN-HIO co-culture model can be used to monitor human

408 genes that are associated with diarrheal responses when infected with *Salmonella* or  
409 other microbial pathogens. Additionally, we show the feasibility of co-culturing HIOs with  
410 immune cells and in the future, this will allow us to add back components incrementally  
411 to model the intestinal environment and individually probe the role of immune cell  
412 subtypes in various pathological conditions. Further characterization of the HIO model  
413 and development of co-culture models of HIOs with immune cells will allow us to more  
414 closely study mechanisms governing the complex human-specific responses of the  
415 intestinal epithelium to bacterial infections.

416

#### 417 **Acknowledgements**

418 This work was supported by the NIH awards U19AI116482-01 (V.B.Y, J.R.S, C.E.W, and  
419 M.X.O) and R21AI13540 (M.X.O). A-L.E.L was supported by NIH T32 AI007528. We  
420 thank the Host Microbiome Initiative, the Comprehensive Cancer Center Immunology  
421 (supported by the NCI and NIH award P30CA046592) and Histology Cores and the DNA  
422 Sequencing Core at University of Michigan Medical School. We gratefully acknowledge  
423 the O’Riordan lab members for helpful discussions, and Dr. Roberto Cieza for assistance  
424 with data management.

425

#### 426 **Author contributions**

427 A-L.E.L and B.H.A performed the experiments and analyzed the data. A-L.E.L, M.X.O  
428 and B.H.A designed the experiments and wrote the manuscript. R.P.B and D.R.H  
429 assisted in RNA-seq analysis. S.H, V.K.Y, B.B and C.F assisted in HIO differentiation and

430 culturing. J.R.S, V.B.Y, C.E.W and J.S.K assisted in experimental preparation and data  
431 interpretation.

432

433 **Declaration of interests**

434 The authors declare no competing interests.

435

436 **Materials and Methods:**

437 **Contact for reagent and resource sharing**

438 All RNA sequences are deposited in the EMBL-EBI Arrayexpress database (E-MTAB-  
439 11089). Source code for RNA-seq analyses can be found at [aelawren/PMN-HIO-RNA-seq: R scripts for PMN-HIO RNA-seq analysis \(github.com\)](https://github.com/aelawren/PMN-HIO-RNA-seq). Other reagents and  
440 resources can be obtained by directing requests to the Lead Contacts, Basel Abuaita  
441 ([babuaita@lsu.edu](mailto:babuaita@lsu.edu)) and Mary O'Riordan ([oriordan@umich.edu](mailto:oriordan@umich.edu)).  
442

443

444 **Experimental model and subject details**

445 **Human Intestinal Organoids (HIOs)**

446 HIOs were generated by the *In Vivo* Animal and Human Studies Core at the University of  
447 Michigan Center for Gastrointestinal Research as previously described (9). Prior to  
448 experiments, HIOs were removed from the Matrigel, washed with DMEM:F12 media, and  
449 re-plated with 5 HIOs/well in 50µl of Matrigel (Corning) in ENR media ((DMEM:F12, 1X  
450 B27 supplement, 2mM L-glutamine, 100ng/ml EGF, 100ng/ml Noggin, 500ng/ml  
451 Rspondin1, and 15mM HEPES). Media was exchanged every 2-3 days for 7 days.

452

453 **Human Polymorphonuclear Leukocytes (PMNs)**

454 PMNs were isolated from blood of healthy human adult donors as previously described  
455 (44), according to the protocol approved by the University of Michigan Medical School  
456 (HUM00044257). Written consent was obtained from all donors. The purity of PMNs was  
457 assessed by flow cytometry using APC anti-CD16 and FITC anti-CD15 antibodies  
458 (Miltenyi Biotec), markers characteristic of human neutrophils.

459

460 **Bacterial Growth and HIO Microinjection**

461 *Salmonella enterica* serovar Typhimurium SL1344 (STM) was used throughout the  
462 manuscript. Bacteria were stored at -80°C in Luria-Bertani (LB, Fisher) medium  
463 containing 20% glycerol and cultured on LB agar plates. Individual colonies were grown  
464 overnight at 37°C under static conditions in LB liquid broth. Bacteria were pelleted,  
465 washed and re-suspended in PBS. Bacterial inoculum was estimated based on OD<sub>600</sub>  
466 and verified by plating serial dilutions on agar plates to determine colony forming units  
467 (CFU). Lumens of individual HIOs were microinjected with glass caliber needles with 1µl  
468 of PBS or STM (10<sup>5</sup> CFU/HIO) as previously described (6, 45, 46). HIOs were then  
469 washed with PBS and incubated for 2h at 37°C in ENR media. HIOs were treated with  
470 100µg/ml gentamicin for 15 min to kill any bacteria outside the HIOs, then incubated in  
471 fresh medium +/- PMNs (5 X 10<sup>5</sup> PMNs/5HIOs/well in a 24-well plate).

472

473 **Method Details**

474 **Cytokine Analyses**

475 For cytokine analysis, media from each well containing 5 HIOs/well were collected at 8hpi.  
476 Cytokines, chemokines and antimicrobial proteins were quantified by ELISA at the  
477 University of Michigan Cancer Center Immunology Core.

478

#### 479 **RNA Sequencing and Analysis**

480 Total RNA was isolated from 5 HIOs per group with a total of 4 replicates per condition  
481 using the mirVana miRNA Isolation Kit (Thermo Fisher). The quality of RNA was  
482 confirmed, ensuring the RNA integrity number (RIN)> 8.5, using the Agilent TapeStation  
483 system. cDNA libraries were prepared by the University of Michigan DNA Sequencing  
484 Core using the TruSeq Stranded mRNA Kit (Illumina) according to the manufacturer's  
485 protocol. Libraries were sequenced on Illumina HiSeq 2500 platforms (single-end, 50 bp  
486 read length). All samples were sequenced at a depth of 10.5 million reads per sample or  
487 greater. Sequencing generated FASTQ files of transcript reads that were pseudoaligned  
488 to the human genome (GRCh38.p12) using kallisto software (47). Transcripts were  
489 converted to estimated gene counts using the tximport package (48) with gene annotation  
490 from Ensembl (49).

491

#### 492 **Gene Expression and Pathway Enrichment Analysis**

493 Differential expression analysis was performed using the DESeq2 package (50) with *P*  
494 values calculated by the Wald test and adjusted *P* values calculated using the Benjamini  
495 & Hochberg method (51). Pathway analysis was performed using the Reactome pathway  
496 database and pathway enrichment analysis in R using the ReactomePA software  
497 package (52).

498

499 **Quantification and Statistical Methods**

500 RNA-seq data analysis was done using RStudio version 1.1.453. Plots were generated  
501 using ggplot2 (53) with data manipulation done using dplyr (54). Euler diagrams of gene  
502 changes were generated using the Eulerr package (55). Other data were analyzed using  
503 Graphpad Prism 9. Statistical differences were determined using statistical tests indicated  
504 in the fig. legends. The mean of at least 2 independent experiments were presented with  
505 error bars showing standard deviation (SD). *P* values of less than 0.05 were considered  
506 significant and designated by: \**P* < 0.05, \*\**P* < 0.01, \*\*\**P* < 0.001 and \*\*\*\* *P* < 0.0001.

507

508 **Supplemental information**

509 **Table S1. Complete list of significant REACTOME pathways with p-value <0.05.**  
510 Genes with p-adjusted value <0.05 and  $\log_2(\text{fold change}) > 0$  relative to PBS-injected  
511 HIOs were selected for analysis.

512

513 **Table S2. Complete list of differentially expressed genes with p-adjusted value of**  
514 **<0.05 compared to PBS-injected HIOs.**

515

516 **Table S3. Complete list of significant REACTOME pathways from genes**  
517 **differentially expressed only in SE-infected PMN-HIOs.** Genes with p-adjusted value  
518 <0.05,  $\log_2(\text{fold change}) > 0$  relative to PBS-injected HIOs and p-adjusted value >0.05 in  
519 STM-infected PMN-HIOs were selected for analysis.

520

521 **Table S4. Complete list of significant REACTOME pathways from genes**  
522 **differentially expressed only in STM-infected PMN-HIOs.** Genes with p-adjusted value  
523 <0.05,  $\log_2(\text{fold change}) > 0$  relative to PBS-injected HIOs and p-adjusted value >0.05 in  
524 SE-infected PMN-HIOs were selected for analysis.

525

526 **References**

527 1. CDC. 2020. Foodborne Germs and Illnesses.  
528 <https://www.cdc.gov/foodsafety/foodborne-germs.html>. Retrieved 10 September  
529 2021.

530 2. 2021. Salmonella Homepage. <https://www.cdc.gov/salmonella/>. Retrieved 10  
531 September 2021.

532 3. Baird-Parker AC. 1990. Foodborne salmonellosis. *Lancet* 336:1231–1235.

533 4. Gilchrist JJ, MacLennan CA. 2019. Invasive Nontyphoidal *Salmonella* Disease in  
534 Africa. *EcoSal Plus* 8.

535 5. Hapfelmeier S, Hardt W-D. 2005. A mouse model for *S. typhimurium*-induced  
536 enterocolitis. *Trends Microbiol* 13:497–503.

537 6. Lawrence A-LE, Abuaita BH, Berger RP, Hill DR, Huang S, Yadagiri VK, Bons B,  
538 Fields C, Wobus CE, Spence JR, Young VB, O'Riordan MX. 2021. *Salmonella*  
539 enterica Serovar Typhimurium SPI-1 and SPI-2 Shape the Global Transcriptional  
540 Landscape in a Human Intestinal Organoid Model System. *MBio* 12.

541 7. Forbester JL, Goulding D, Vallier L, Hannan N, Hale C, Pickard D, Mukhopadhyay  
542 S, Dougan G. 2015. Interaction of *Salmonella enterica* Serovar Typhimurium with  
543 Intestinal Organoids Derived from Human Induced Pluripotent Stem Cells. *Infect*  
544 *Immun* 83:2926–2934.

545 8. Abuaita BH, Lawrence A-LE, Berger RP, Hill DR, Huang S, Yadagiri VK, Bons B,  
546 Fields C, Wobus CE, Spence JR, Young VB, O'Riordan MX. 2021. Comparative  
547 transcriptional profiling of the early host response to infection by typhoidal and non-  
548 typhoidal *Salmonella* serovars in human intestinal organoids. *PLoS Pathog*  
549 17:e1009987.

550 9. Spence JR, Mayhew CN, Rankin SA, Kuhar MF, Vallance JE, Tolle K, Hoskins EE,  
551 Kalinichenko VV, Wells SI, Zorn AM, Shroyer NF, Wells JM. 2011. Directed  
552 differentiation of human pluripotent stem cells into intestinal tissue in vitro. *Nature*  
553 470:105–109.

554 10. Hill DR, Huang S, Nagy MS, Yadagiri VK, Fields C, Mukherjee D, Bons B, Dedhia  
555 PH, Chin AM, Tsai Y-H, Thodla S, Schmidt TM, Walk S, Young VB, Spence JR. 2017.  
556 Bacterial colonization stimulates a complex physiological response in the immature  
557 human intestinal epithelium. *Elife* 6.

558 11. Karve SS, Pradhan S, Ward DV, Weiss AA. 2017. Intestinal organoids model human  
559 responses to infection by commensal and Shiga toxin producing *Escherichia coli*.  
560 *PLoS One* 12:e0178966.

561 12. Pradhan S, Weiss AA. 2020. Probiotic Properties of *Escherichia coli* Nissle in Human  
562 Intestinal Organoids. *MBio* 11.

563 13. Schulte LN, Schweinlin M, Westermann AJ, Janga H, Santos SC, Appenzeller S,  
564 Walles H, Vogel J, Metzger M. 2020. An Advanced Human Intestinal Coculture Model  
565 Reveals Compartmentalized Host and Pathogen Strategies during *Salmonella*  
566 Infection. *MBio* 11.

567 14. Hannemann S, Galán JE. 2017. *Salmonella enterica* serovar-specific transcriptional  
568 reprogramming of infected cells. *PLoS Pathog* 13:e1006532.

569 15. Hannemann S, Gao B, Galán JE. 2013. *Salmonella* modulation of host cell gene  
570 expression promotes its intracellular growth. *PLoS Pathog* 9:e1003668.

571 16. Rydström A, Wick MJ. 2007. Monocyte recruitment, activation, and function in the  
572 gut-associated lymphoid tissue during oral *Salmonella* infection. *J Immunol*  
573 178:5789–5801.

574 17. Tükel C, Raffatellu M, Chessa D, Wilson RP, Akçelik M, Bäumler AJ. 2006.  
575 Neutrophil influx during non-typhoidal salmonellosis: who is in the driver's seat?  
576 *FEMS Immunol Med Microbiol* 46:320–329.

577 18. Amulic B, Cazalet C, Hayes GL, Metzler KD, Zychlinsky A. 2012. Neutrophil function:  
578 from mechanisms to disease. *Annu Rev Immunol* 30:459–489.

579 19. Brinkmann V, Reichard U, Goosmann C, Fauler B, Uhlemann Y, Weiss DS,  
580 Weinrauch Y, Zychlinsky A. 2004. Neutrophil extracellular traps kill bacteria. *Science*  
581 303:1532–1535.

582 20. Campbell EL, Bruyninckx WJ, Kelly CJ, Glover LE, McNamee EN, Bowers BE,  
583 Bayless AJ, Scully M, Saeedi BJ, Golden-Mason L, Ehrentraut SF, Curtis VF,  
584 Burgess A, Garvey JF, Sorensen A, Nemenoff R, Jedlicka P, Taylor CT, Kominsky  
585 DJ, Colgan SP. 2014. Transmigrating neutrophils shape the mucosal  
586 microenvironment through localized oxygen depletion to influence resolution of  
587 inflammation. *Immunity* 40:66–77.

588 21. Fournier BM, Parkos CA. 2012. The role of neutrophils during intestinal inflammation.  
589 *Mucosal Immunol* 5:354–366.

590 22. Lawrence A-LE, Berger RP, Hill DR, Huang S, Yadagiri VK, Bons B, Fields C, Sule  
591 GJ, Knight JS, Wobus CE, Spence JR, Young VB, O’Riordan MX, Abuaita BH. 2022.  
592 Human neutrophils direct epithelial cell extrusion to enhance intestinal epithelial host  
593 defense during *Salmonella* infection. *bioRxiv*.

594 23. Patel JC, Galán JE. 2005. Manipulation of the host actin cytoskeleton by *Salmonella*-  
595 -all in the name of entry. *Curr Opin Microbiol* 8:10–15.

596 24. Rouillard AD, Gundersen GW, Fernandez NF, Wang Z, Monteiro CD, McDermott  
597 MG, Ma’ayan A. 2016. The harmonizome: a collection of processed datasets  
598 gathered to serve and mine knowledge about genes and proteins. *Database* 2016.

599 25. Sumagin R, Parkos CA. 2015. Epithelial adhesion molecules and the regulation of  
600 intestinal homeostasis during neutrophil transepithelial migration. *Tissue Barriers*  
601 3:e969100.

602 26. Andrews C, McLean MH, Durum SK. 2018. Cytokine Tuning of Intestinal Epithelial  
603 Function. *Front Immunol* 9:1270.

604 27. Wang D, Dubois RN, Richmond A. 2009. The role of chemokines in intestinal  
605 inflammation and cancer. *Curr Opin Pharmacol* 9:688–696.

606 28. Ray S, Das S, Panda PK, Suar M. 2018. Identification of a new alanine racemase in  
607 *Salmonella Enteritidis* and its contribution to pathogenesis. *Gut Pathog* 10:30.

608 29. Silva CA, Blondel CJ, Quezada CP, Porwollik S, Andrews-Polymenis HL, Toro CS,  
609 Zaldívar M, Contreras I, McClelland M, Santiviago CA. 2012. Infection of mice by  
610 *Salmonella enterica* serovar Enteritidis involves additional genes that are absent in  
611 the genome of serovar Typhimurium. *Infect Immun* 80:839–849.

612 30. Dhanani AS, Block G, Dewar K, Forgetta V, Topp E, Beiko RG, Diarra MS. 2016.  
613 Correction: Genomic Comparison of Non-Typhoidal *Salmonella enterica* Serovars  
614 Typhimurium, Enteritidis, Heidelberg, Hadar and Kentucky Isolates from Broiler  
615 Chickens. *PLoS One* 11:e0148706.

616 31. Caruso JA, Akli S, Pageon L, Hunt KK, Keyomarsi K. 2015. The serine protease  
617 inhibitor elafin maintains normal growth control by opposing the mitogenic effects of  
618 neutrophil elastase. *Oncogene* 34:3556–3567.

619 32. Pazgier M, Hoover DM, Yang D, Lu W, Lubkowski J. 2006. Human beta-defensins.  
620 Cell Mol Life Sci 63:1294–1313.

621 33. Jukic A, Bakiri L, Wagner EF, Tilg H, Adolph TE. 2021. Calprotectin: from biomarker  
622 to biological function. Gut 70:1978–1988.

623 34. Reid PT, Marsden ME, Cunningham GA, Haslett C, Sallenave JM. 1999. Human  
624 neutrophil elastase regulates the expression and secretion of elafin (elastase-  
625 specific inhibitor) in type II alveolar epithelial cells. FEBS Lett 457:33–37.

626 35. Santos AJM, Meinecke M, Fessler MB, Holden DW, Boucrot E. 2013. Preferential  
627 invasion of mitotic cells by *Salmonella* reveals that cell surface cholesterol is maximal  
628 during metaphase. J Cell Sci 126:2990–2996.

629 36. Misselwitz B, Dilling S, Vonaesch P, Sacher R, Snijder B, Schlumberger M, Rout S,  
630 Stark M, von Mering C, Pelkmans L, Hardt W-D. 2011. RNAi screen of *Salmonella*  
631 invasion shows role of COPI in membrane targeting of cholesterol and Cdc42. Mol  
632 Syst Biol 7:474.

633 37. Nawabi P, Catron DM, Haldar K. 2008. Esterification of cholesterol by a type III  
634 secretion effector during intracellular *Salmonella* infection. Mol Microbiol 68:173–  
635 185.

636 38. Greene AR, Owen KA, Casanova JE. 2021. *Salmonella Typhimurium* manipulates  
637 macrophage cholesterol homeostasis through the SseJ-mediated suppression of the  
638 host cholesterol transport protein ABCA1. Cell Microbiol 23:e13329.

639 39. Catron DM, Lange Y, Borensztajn J, Sylvester MD, Jones BD, Haldar K. 2004.

640        *Salmonella enterica* serovar *Typhimurium* requires nonsterol precursors of the

641        cholesterol biosynthetic pathway for intracellular proliferation. *Infect Immun* 72:1036–

642        1042.

643 40. Gilk SD, Cockrell DC, Luterbach C, Hansen B, Knodler LA, Ibarra JA, Steele-

644        Mortimer O, Heinzen RA. 2013. Bacterial colonization of host cells in the absence of

645        cholesterol. *PLoS Pathog* 9:e1003107.

646 41. Rotimi SO, Ojo DA, Talabi OA, Balogun EA, Ademuyiwa O. 2012. Tissue

647        dyslipidemia in *Salmonella*-infected rats treated with amoxillin and pefloxacin. *Lipids*

648        *Health Dis* 11:152.

649 42. Huang F-C. 2014. The critical role of membrane cholesterol in *salmonella*-induced

650        autophagy in intestinal epithelial cells. *Int J Mol Sci* 15:12558–12572.

651 43. Alvarez MI, Glover LC, Luo P, Wang L, Theusch E, Oehlers SH, Walton EM, Tram

652        TTB, Kuang Y-L, Rotter JI, McClean CM, Chinh NT, Medina MW, Tobin DM, Dunstan

653        SJ, Ko DC. 2017. Human genetic variation in *VAC14* regulates *Salmonella* invasion

654        and typhoid fever through modulation of cholesterol. *Proc Natl Acad Sci U S A*

655        114:E7746–E7755.

656 44. Abuaita BH, Sule GJ, Schultz TL, Gao F, Knight JS, O'Riordan MX. 2021. The IRE1 $\alpha$

657        Stress Signaling Axis Is a Key Regulator of Neutrophil Antimicrobial Effector

658        Function. *J Immunol* <https://doi.org/10.4049/jimmunol.2001321>.

659 45. Abuaita BH, Lawrence A-LE, Berger RP, Hill DR, Huang S, Yadagiri VK, Bons B,  
660 Fields C, Wobus CE, Spence JR, Young VB, O'Riordan MX. 2020. Comparative  
661 transcriptional profiling of the early host response to infection by typhoidal and non-  
662 typhoidal *Salmonella* serovars in human intestinal organoids. *bioRxiv*.

663 46. Hill DR, Huang S, Tsai Y-H, Spence JR, Young VB. 2017. Real-time Measurement  
664 of Epithelial Barrier Permeability in Human Intestinal Organoids. *J Vis Exp*  
665 <https://doi.org/10.3791/56960>.

666 47. Bray NL, Pimentel H, Melsted P, Pachter L. 2016. Near-optimal probabilistic RNA-  
667 seq quantification. *Nat Biotechnol* 34:525–527.

668 48. Soneson C, Love MI, Robinson MD. 2015. Differential analyses for RNA-seq:  
669 transcript-level estimates improve gene-level inferences. *F1000Res* 4:1521.

670 49. Rainer J. 2017. EnsDb.Hsapiens.v75: Ensembl based annotation package. R  
671 package version 2.99.0.

672 50. Love MI, Huber W, Anders S. 2014. Moderated estimation of fold change and  
673 dispersion for RNA-seq data with DESeq2. *Genome Biol* 15:550.

674 51. Benjamini Y, Hochberg Y. 1995. Controlling the False Discovery Rate: A Practical  
675 and Powerful Approach to Multiple Testing. *Journal of the Royal Statistical Society:*  
676 *Series B (Methodological)* <https://doi.org/10.1111/j.2517-6161.1995.tb02031.x>.

677 52. Yu G, He Q-Y. 2016. ReactomePA: an R/Bioconductor package for reactome  
678 pathway analysis and visualization. *Mol Biosyst* 12:477–479.

679 53. Wickham H. 2016. *ggplot2: Elegant Graphics for Data Analysis*. Springer.

680 54. Wickham H, Francois R, Henry L, Müller K, Others. 2015. *dplyr: A grammar of data*  
681 *manipulation*. R package version 0.4.3.

682 55. Larsson J. 2019. *eulerr: Area-Proportional Euler and Venn Diagrams with Ellipses* (R  
683 package version 5.1.0).